Biosensors and Bioelectronics 144 (2019) 111630

Contents lists available at ScienceDirect

Biosensors and Bioelectronics

journal homepage: www.elsevier.com/locate/bios

Tuning *Geobacter sulfurreducens* biofilm with conjugated polyelectrolyte for increased performance in bioelectrochemical system

Lijiao Ren, Samantha R. McCuskey, Alex Moreland, Guillermo C. Bazan, Thuc-Quyen Nguyen*

Center for Polymers and Organic Solids, Department of Chemistry and Biochemistry, University of California, Santa Barbara, Santa Barbara, CA, 93106, USA

ARTICLE INFO

Keywords:
Conjugated polyelectrolyte
Bioelectrochemical system
Geobacter sulfurreducens
Current production
Biomass content
Biofilm permeability

ABSTRACT

Bioelectrochemical systems (BESs) are emerging as a platform technology with great application potentials such as wastewater remediation and power generation. Materials for electrode/microorganism modification are being examined in order to improve the current production in BESs. Herein, we report that the current production increased almost one fold in single-chamber BES reactors, by adding a conjugated polyelectrolyte (CPE-K) in the growth medium to co-form the anodic biofilm with *Geobacter sulfurreducens* cells. The CPE-K treated BESs had a maximum current density as high as 12.3 ± 0.5 A/m^2, with that of the controls being 6.2 ± 0.7 A/m^2. Improved current production was sustained even after CPE-K was no longer added to the medium. It was demonstrated that increased current resulted from improvement of certain biofilm properties. Analysis using electrochemical impedance spectroscopy (EIS) showed that CPE-K addition decreased the charge transfer resistance at the cell/electrode interface and the diffusion resistance through the biofilm. Protein quantification showed increased biomass growth on the electrode surface, and confocal scanning microscopy images revealed enhanced biofilm permeability. These results demonstrated for the first time that conjugated polyelectrolytes could be used for *G. sulfurreducens* biofilm augmentation to achieve high electricity production through tuning the anodic biofilm in BESs.

1. Introduction

Increasing awareness of the energy-environment nexus is compelling the development of technologies that reduce environmental impacts during energy generation as well as energy consumption during environmental remediation (Wang et al., 2015). Bioelectrochemical systems (BESs) are emerging as a platform technology for many potential applications in sustainable energy production and environmental protection, including electricity generation, hydrogen production, and wastewater treatment (Ivanov et al., 2013; Logan and Rabaey, 2012; Olabi, 2012, 2013, 2014). In these devices, the microorganisms function as catalysts to extracellularly transfer electrons to the electrode (Logan and Rabaey, 2012; Lovley, 2012). The electron transfer between cells and at the cell/electrode interface is critical for the functional activity of the bio-catalyst and thus the BES performance (Logan and Rabaey, 2012; Lovley, 2012; Logan, 2009). Materials for electrode/microorganism modification strategies are thus being examined in order to improve extracellular electron transfer from exoelectrogenic microorganisms to the electrode. Examples include carbon based electrode materials modified with metal oxide nanoparticles (Kumar et al., 2016), redox polymers (Patil et al., 2012), traditional conducting polymers such as polyaniline (PANI) and polypyrrole (PPy) (Li et al., 2017), and membrane-intercalating conjugated oligoelectrolytes (COEs) (Kirchhofer et al., 2017a). In general, optimal performance is achieved by a modified electrode surface that fosters microorganism adhesion and growth. There are also studies using chemical treatments such as surfactant (Wen et al., 2011), staining cells with COEs (Hou et al., 2013), or adding conductive nano-particles such as magnetite (Kato et al., 2012), to increase the cell membrane permeability or biofilm conductivity, and thus achieve better performance of the BESs.

Recently, ionic liquid polymers (ILPs) as a new type of polymer material have been widely used as polyelectrolyte in electrochemical devices (Armand et al., 2009; Le Bideau et al., 2011; Yang et al., 2014), and also showed promising results for application in BESs. The current generation in microbial fuel cells (MFCs) was boosted by coating a hydrophilic and positively charged ILP on carbon-based-electrodes, as a result of increased bacterial loading capacity and improved mediated extracelluar electron transfer between the electrode and *Shewanella putrefaciens* cells (Yang et al., 2017). A self-doped conjugated polyelectrolyte (CPE-K) was shown to be able to function as an electron acceptor from *Shewanella oneidensis* MR-1 (Kirchhofer et al., 2017b). Microbial three-electrode electrochemical cells (M3Cs) also showed an

* Corresponding author.
E-mail address: quyen@chem.ucsb.edu (T.-Q. Nguyen).

https://doi.org/10.1016/j.bios.2019.111630
Received 20 May 2019; Received in revised form 17 August 2019; Accepted 22 August 2019
Available online 28 August 2019
0956-5663/ © 2019 Elsevier B.V. All rights reserved.

increase in current generated by *S. oneidensis* MR-1 with addition of CPE-K by promoting the coverage of a cell monolayer on the carbon fiber electrode (Kirchhofer et al., 2017b).

The improved bioelectrochemcial performance by polyelectrolytes modification was demonstrated with *Shewanella* species, a weak exoelectrogenic bacterium. As a model exoelectrogenic bacterium, *S. oneidensis* is known to produce a thin biofilm (< 10 μm) (Lanthier et al., 2008; Malvankar and Lovely, 2015) and thus produces relatively low current in BES. In contrast, *Geobacter sulfurreducens*, another model exoelectrogenic bacterium, is capable of forming a thick (> 40 μm), conductive biofilm on electrode surfaces and is thus able to produce high currents (Malvankar et al., 2012; Nevin et al., 2008). It is assumed in some studies that the high electrochemical activity of *G. sulfurreducens* is positively correlated with the biofilm thickness or the total biomass (Lovley, 2012; Franks et al., 2010; Guo et al., 2013). Other studies show that the operational current of *G. sulfurreducens* in BESs stabilizes with newborn thin biofilm, while further growth of biofilm cannot improve the current output (Bond and Lovley, 2003; Call et al., 2009; Cheng et al., 2011; Zhang et al., 2011b). Moreover, the electrochemical activity of the aged biofilm will decrease due to the large diffusion resistance through the thick biofilm (Renslow et al., 2013; Sun et al., 2016). For a thick biofilm, the rate of catalytic electron generation by the exoelectrogens can be limited by mass transport of substrate into the biofilm or insufficient rate of proton transport out of the biofilm. Due to these intrinsic differences in terms of biofilm morphology and current producing ability between *G. sulfurreducens* and *S. oneidensis*, it is worth examinining the effect of CPE-K on *G. sulfurreducens* biofilms and current generation in BESs.

To demonstrate the electrode- or microorganism-modification strategies for improved current production in BESs, most studies use weakly exoelectrogenic microorganisms or undefined mixed cultures as inoculum and test for a short period of time. In such cases, the current production of the control (unmodified electrode) itself is quite low. It is of interest to know the outcome of any modification strategies during stable performance or even in long-term operation. In order to better understand the effect of CPE-K on exoelectrogenic biofilms, we examined the operational current produced in BES, the biomass content, and the metabolic activity of *G. sulfurreducens* biofilms with CPE-K modification by comparison with control systems. The examinations were conducted at start-up stage (initial 10 cycles), during stable performance (11–20 cycles), and after stopping CPE-K addition (21–26 cycles). Different poised anode potentials (0 V and +0.3 V versus Ag/AgCl reference electrode) and CPE-K concentrations (10 μM and 100 μM) were tested.

2. Material and methods

2.1. Reactor construction and operation

Single chambered BES reactors were constructed using 20 mL clear glass scintillation vials (Wheaton™) sealed with serrated silicone rubber septa (Sigma-Aldrich, bottom O.D. 18 mm, Sure/Seal) (Supplemental information, Fig. S1). The anode was built as described previously (Call and Logan, 2011), using a graphite plate with a thickness of 0.32 cm and dimensions of 2.5 cm × 1.5 cm (Grade GM-10; GraphiteStore.com, Inc.). All anodes were polished using sandpaper (grit type 1500), sonicated to remove debris, cleaned by soaking consecutively in 1 M NaOH and 1 M HCl overnight, and rinsed three times in Milli-Q water. The cathode was titanium wire (0.8 cm diameter; McMaster-Carr), cleaned with sand paper (grit type 400) and coiled 10 turns. The anode potential was controlled using a Gamry potentiostat (Reference 600, Series G300 models) and multiplexer (model ECM8), with the anode as the working electrode and the cathode as the counter electrode. Reference electrode (Ag/AgCl in 3 M NaCl; BASi) was used to set the anode potential by inserting the electrode (0.57 cm diameter) through a hole cut in the silicone septa (0.5 cm diameter), with the tip placed between the anode and the cathode. All electrode potential values were reported here versus Ag/AgCl [+200 mV vs standard hydrogen electrode (SHE)].

Reactors were autoclaved and sparged with filtered (Target2™ PTFE Syringe Filters, pore size 0.2 μm) anaerobic gas (CO_2/N_2, [20/80]) before inoculation. Cell suspension of *G. sulfurreducens* was prepared from a stock culture as previously described (Call et al., 2009), in an acetate (10 mM) growth medium using fumarate (40 mM) as the electron acceptor. BESs were inoculated with *G. sulfurreducens* in the late exponential growth phase using 7.5 mL of the cell suspension and 7.5 mL of growth medium. Growth medium was made in fresh water buffer (ATCC 2260) containing (per liter) 10 mM CH_3COONa, 0.25 g NH_4Cl, 0.06 g NaH_2PO_4, 0.1 g KCl, 2.5 g $NaHCO_3$, 10 mL Wolf's vitamins solution, and 10 mL Wolf's minerals solution (Balch et al., 1979). The growth medium was sparged with CO_2/N_2 [20/80] for 30 min, autoclaved, and stored in 125 mL sealed serum bottles. Reactors were operated in fed-batch mode, with medium replacement after the current dropped below 0.5 mA. A cycle is defined as the time period between each medium replacement. The multiplexer channels were programmed with the same sample and block time, to operate up to eight BES reactors simultaneously at the same electrochemical condition except the anode potentials (0 V or +0.3 V versus Ag/AgCl reference electrode). Four trials were conducted to comprehensively examine the effect of CPE-K at different concentrations and anode poised potentials (Supplemental information, Table S1). All tests were conducted in a temperature controlled incubator at 30 °C.

2.2. Chemical and electrochemical analyses

All chemicals were purchased from Fisher Scientific or Sigma Aldrich and used as received unless otherwise indicated. CPE-K was synthesized according to literature procedures (Mai et al., 2013) and its structure was shown in Fig. S2 (Supplemental information). CPE-K was p-doped in aqueous media at pH > 6, and its oxidation potential fell at +0.27 V versus Ag/AgCl (Mai et al., 2013; Kirchhofer et al., 2017b). CPE-K was added starting from the inoculation of the BESs at 10 μM or 100 μM final concentration and in every cycle with growth medium refreshment, by first making concentrated aqueous solutions (2 mM in Milli-Q water) and then adding the necessary negligible volume of the stock solutions to achieve the final concentration. pH was measured using a probe (InLab®Versatile, Mettler-ToledoInternational Inc.) connected to a pH meter (SevenEasy S20, Mettler-ToledoInternational Inc.). Biomass was measured based on the protein content extracted from the entire anode as describe previously (Li et al., 2015). The protein content was quantified using the Coomassie (Bradford) Protein Assay Kit (Thermo Scienfitic) following the manufacture's procedure. Confocal scanning microscopy (Leica SP8 Resonant Scanning Confocal) was conducted with a water objective (40x/1.1 water motorized correction collar), and the three dimensional biofilm status (z-stack) was reconstructed and analyzed by the software of Leica Application Suite X (Edition 3.1.1.15751). The viability of the cells was observed by staining the biofilms with DAPI and propidium iodide, and the permeability of the biofilm was traced based on the diffusion of fluorescein with 5 min staining and 1 h incubation.

The current was reported at 5 minutes intervals, with current density (A/m^2) normalized to the anode projected surface area of 3.75 cm^2. Half-cell electrochemical impedance spectroscopy (EIS) was conducted in the same BES reactor in the same medium used for biofilm growth, with the anode as working electrode, the cathode as the counter electrode, and a Ag/AgCl reference electrode located between the working and the counter electrode. The polarized condition was chosen to be close to BES operating potential, which were 0 V for the anode. The frequency range was 100 kHz to 10 mHz with a sinusoidal perturbation of 10 mV amplitude (Zhang et al., 2011a). EIS spectra were fitted to an equivalent circuit (Supplemental information, Fig. S3) (Sun et al., 2016), based on the flooded-agglomerate model (Zhang et al., 2011a;

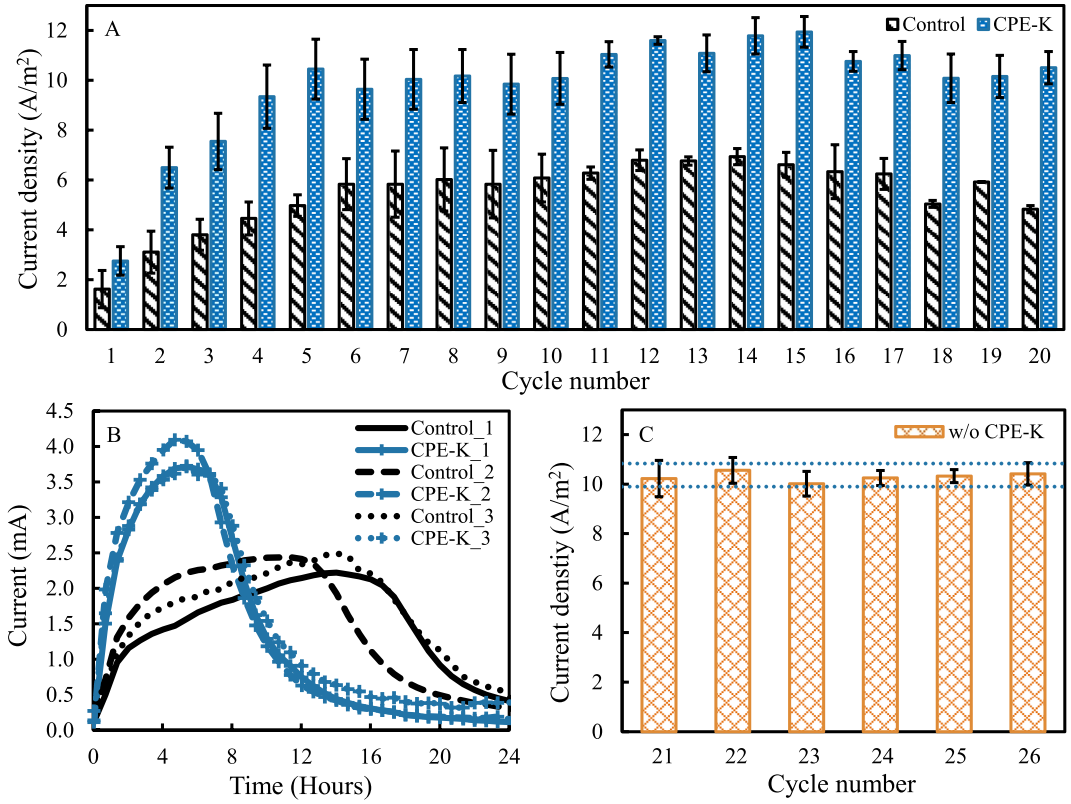

Fig. 1. Current production by *G. Sulfurreducens* in BESs with CPE-K addition and the controls at start-up stage (initial 10 cycles), during stable performance (11–20 cycles), and after stopping CPE-K addition (21-26 cycles). (A) The maximum current density at start-up and during stable performance; (B) current profiles of a typical cycle during stable performance; (C) the maximum current density after stopping CPE-K addition. The values reported in (A) and (C) are the averaged maximum values for CPE-K added BESs and the controls in each cycle as that shown in (B). The error bars in (A) stand for the standard deviations of triplicates. The error bars in (C) stand for the standard deviations of two BESs with previous CPE-K treatment. The dotted lines in (C) indicate the highest and lowest maximum current density of the two CPE-K treated BESs in cycle 16 to 20 in (A).

Springer and Raistrick, 1989), to extract the Ohmic, charge transfer, and diffusion resistances. A constant phase element (Q) was used instead of a capacitor in order to adapt to nonhomogeneous conditions, such as electrode roughness and distributed reaction rates (Zhang et al., 2011a; Springer and Raistrick, 1989).

3. Results

3.1. Increqased current density with CPE-K addition

Six BES reactors were operated with anode potential poised at 0 V versus Ag/AgCl reference electrode and CPE-K was added into three of them at a concentration of 10 μM every time with medium refreshment from the start-up while the rest were left as controls. The maximum current dentsity of the six reactors increased rapidly in the initial five cycles, and then gradually increased in the following 5 cycles (Fig. 1A). The cycle time was 3 days for the first cycle, 2 days for the second and the third, and 1 day for the remaining cycles. All of the reactors reached stable performance in 10 cycles (15 days), indicated by comparable current production over three consecutive cycles. Subsequently, all of the reactors were operated for ten more cycles, with the duration of each cycle being one day. At stable performance (11–20 cycles), the maximum current density produced by the BESs with CPE-K addition was 11.0 ± 0.6 A/m^2 (cycle 15), while that of the controls was 6.2 ± 0.7 A/m^2 (cycle 14) (Fig. 1A). The maximum current density increased by 77% with CPE-K addition compared with that of the controls. By the end of the stable performance (cycle 16 to 20), slightly decreased maximum current density was observed for both CPE-K treated BESs (10.5 ± 0.4 A/m^2) and the controls (5.7 ± 0.7 A/m^2) (Fig. 1A). This was most probably due to aging of the biofilms, as it had been reported previously that the electrochemical activity of aged biofilms decreased (Renslow et al., 2013; Sun et al., 2016). However, the maximum current density of the aged BESs with CPE-K addition was still 84% higher than that of the controls.

The current profiles of the six BES reactors in a typical cycle during the stable performance is shown in Fig. 1B. The current increased rapidly to about half of the maximum current in the first couple of hours after changing to fresh medium. Then, the increase of current slowed down until a maxima was reached, at which point the current started to decrease due to depletion of substrate (Fig. 1B). The current increased faster in BESs with CPE-K addition and reached the maximum at around 6 h, compared to the controls with maximum current achieved at 13–15 h (Fig. 1B). With CPE-K addition, the *G. sulfurreducens* biofilm showed enhanced capability in terms of producing higher current. In a cycle, the total coulombs collected was 131 ± 6 C for the BESs with CPE-K addition and 138 ± 15 C for the controls, with COD (Chemical Oxygen Demand) removals being 541 ± 8 mg/L and 547 ± 7 mg/L, respectively. These results indicate that the presence of CPE-K had no effect on columbic recovery and substrate utilization by *G. sulfurreducens* in BESs. At the end of a cycle, the pH in the CPE-K added BESs was 7.6 ± 0.2 and that of the controls was 7.5 ± 0.1. Thus, the increased current production was not attributed to the difference in medium pH resulting from the addition of CPE-K.

At the end of cycle 20 in Fig. 1A, two of the BESs treated with CPE-K were fed medium without CPE-K for six more cycles (21–26 cycles), while the rest were terminated for other measurements. Without additional CPE-K in the replacement medium, these two BESs produced a maximum current density of 10.3 ± 0.2 A/m^2 over the next six cycles (Fig. 1C), the same as that measured during the CPE-K addition phase (10.5 ± 0.4 A/m^2, cycle 16 to 20 in Fig. 1A). Although all of the BESs

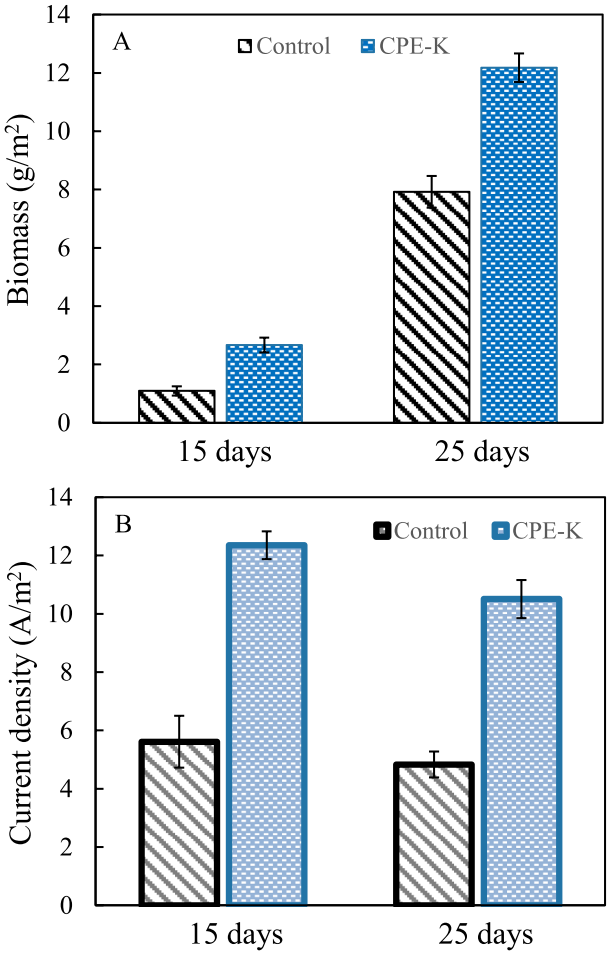

Fig. 2. Biomass content (A) and maximum current density (B) of *G. Sulfurreducens* biofilm in BESs with CPE-K addition and the controls at different operational stages. The error bars stand for the standard deviations of the duplicate with CPE-K addition and the controls.

showed slightly decreased current production by the end of the stable performance stage (Fig. 1A), the maximum current density of the CPE-K treated BESs did not further decrease even after six more cycles of operation without CPE-K addition (Fig. 1C). Once the *G. sulfurreducens* biofilms were mature in the presence of CPE-K, no further CPE-K addition was required to sustain the increased current production and the stability of the biofilm.

3.2. Increased biomass growth with CPE-K addition

Biomass of the anode biofilms were measured for two controls and one CPE-K treated BES at the end of cycle 20 in Fig. 1A, with another CPE-K treated one measured at the end of cycle 26 in Fig. 1C, both in the stable performance stage (25 days). Another batch of BESs were operated with two CPE-K treated ones and two controls, and sacrified for biomass quatification at the end of the start-up stage (15 days). For both operational stages, it was clear that the biomass content of *G. sulfurreducens* biofilms with CPE-K addition was higher than those of the controls (Fig. 2A), exhibiting a similar trend with that of the maximum current density (Fig. 2B). At 15 days, the biomass of the CPE-K treated BESs was 2.7 g/m^2, almost 2.5-fold that of the controls (1.1 ± 0.1 g/m^2); while the maximum current of the CPE-K treated BESs was 12.3 ± 0.5 A/m^2, being 2.1-fold that of the controls (5.9 ± 0.9 A/m^2). Similarly, at 25 days the biomass content of BESs with CPE-K addition (12.1 ± 0.2 g/m^2) was higher than that of the controls (7.9 ± 0.3 g/m^2) (Fig. 2A), and the maximum current density also followed this trend with 10.5 ± 0.6 A/m^2 for the CPE-K treated ones and 5.2 ± 0.4 A/m^2 for the controls (Fig. 2B).

At the end of the start-up stage (15 days), the biomass content of both the CPE-K treated BES and the controls was in the range where the current density should increase with biomass, as transportation of substrate or metabolic products was not the limiting factor in these thin biofilm (Sun et al., 2016). Thus, the BES with CPE-K addition produced higher maximum current density at the start-up stage (Figs. 1A and 2B) as a result of the increased biomass growth of *G. sulfurreducens* biofilms. During the stable performance stage, the increased maximum current density produced by the CPE-K supplemented BESs could also be attributed to the increased biomass content compared to the controls. However, the maximum current density produced by the *G. sulfurreducens* biofilms grown for 25 days was comparable to or even lower than that of the 15-day old biofilm, for both with CPE-K addition and the controls (Fig. 2B), even though with longer acclimation time there was much higher biomass (Fig. 2A). The stagnation of the maximum current density with increasing biomass could be attributed to increased charge transfer and diffusion resistance caused by thickening of the biofilm (Sun et al., 2016). Therefore, it is unclear why the BESs with CPE-K addition produced higher maximum current density even with excessive accumulation of biomass in matured biofilm after 25 days of operation. This indicatied that other current-producing-related aspects of the biofilm had been altered by CPE-K addition rather than just the enhanced biomass growth.

3.3. Electrochemical tests

The components of the anodic internal resistance were examined using EIS (electrochemical impedance spectroscopy) for all six BES reactors at the end of cycle 20 in Fig. 1A. The solution resistance was identical between the BESs with CPE-K addition (21 ± 3 Ω) and the controls (23 ± 1 Ω) (Fig. 3A), indicating that adding CPE-K did not affect the conductivity of the medium which was expected based on the trival amount of only 10 μM added. The anodes with *G. sulfurreducens* biofilm formed in the presence of CPE-K had a much smaller charge transfer resistance (4 ± 1 Ω) at the electrode interface, compared with the controls (20 ± 9 Ω) (Fig. 3A). This decreased charge transfer resistance could result from enhanced attachment of the *G. sulfurreducens* cells onto the carbon-based electrode surface and thus better electronic coupling at the cell/electrode interface. A previous study also showed that CPE-K could promote the coverage of a monolayer of *S. oneidensis* MR-1 cells on a carbon fiber electrode (Kirchhofer et al., 2017b). However, the anodic charge transfer resistance through the CPE-K treated biofilm was 400 ± 100 Ω, almost two times of that of the controls (226 ± 100 Ω) (Fig. 3A). Similarly, the diffusion resistance of 930 ± 60 Ω with CPE-K addition was also larger than that (790 ± 150 Ω) of the controls, but by a smaller extent of 20% (Fig. 3A). In general, it is believed that the lower the resistance is, the higher the electrochemical activity is, and thus the higher the operational current is. However, the total anodic resistance with CPE-K addition (1355 Ω) was larger than that of the controls (1059 Ω), which was contradictory to the increased current production in the CPE-K treated BESs (Fig. 1A).

During the initial phase of biofilm growth, the charge transfer resistance has been shown to decrease with increase in biofilm thickness (biofilm biomass), while the diffusion resistance increased (Nevin et al., 2008). For mature biofilm, both the charge transfer resistance and diffusion resistance could increase with the accumulation of biomass (Sun et al., 2016). Taking into account that the biomass content of the BESs with CPE-K addition was 1.5-times of that of the control at 25 day (Fig. 2A), it made sense that the CPE-K treated BESs had larger charge transfer and diffusion resistance through the biofilm (Fig. 3A). In order to resolve this issue and make a fair comparison, the charge transfer and diffusion resistance through the biofilm were normalized by the biomass content and called “specific resistance” (Fig. 3B). The specific

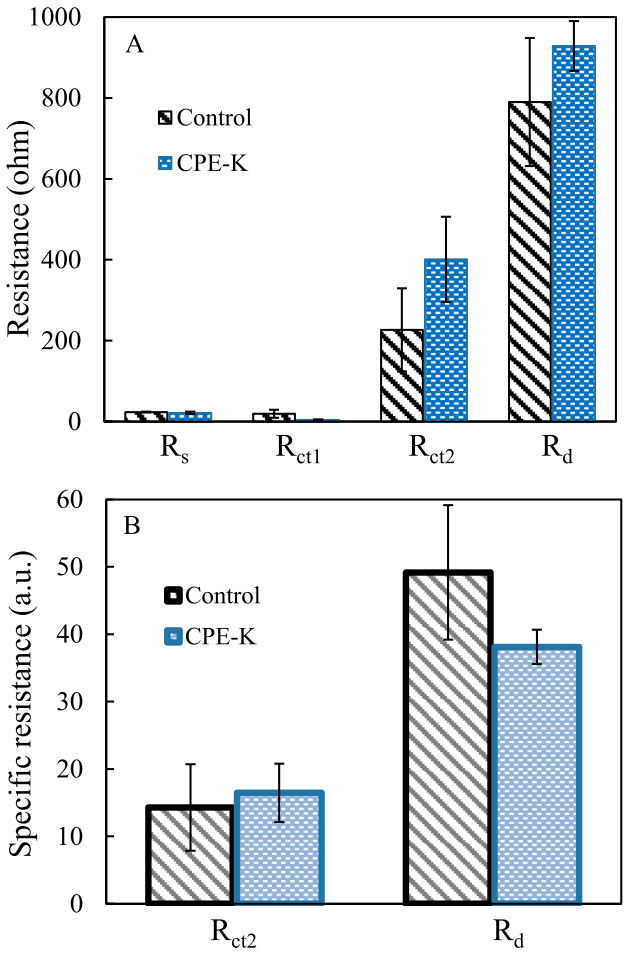

Fig. 3. Fitted resistances (solution resistance, R_s; charge transfer resistance at the biofilm and graphite electrode interface, R_{ct1}; charge transfer resistance through the biofilm, R_{ct2}; and diffusion resistance, R_d) of *G. sulfurreducens* biofilm with CPE-K addition and the controls (A). The specific resistance (B) was the fitted resistance divided by the biomass content, and "a. u." stands for arbitrary unit. Example of EIS plots and fits were shown in Fig. S4 (Supplementary information). The error bars stand for the standard deviations of triplicates with CPE-K addition and of the controls.

charge transfer resistance was comparable between the anodes with CPE-K addition (16 ± 4) and the controls (14 ± 6). Notably, the specific diffusion resistance (38 ± 2) of the CPE-K treated anodes was lower than that (49 ± 9) of the controls by 25% (Fig. 3B). This indicated that the presence of CPE-K inside the *G. sulfurreducens* biofilm also helped to mitigate the diffusion resistance.

3.4. Spatial cell viability and biofilm permeability

The *G. sulfurreducens* biofilms with CPE-K addition and the controls were stained to examine the Live/Dead viability and the total biofilm thickness. The 3D metabolic status images showed that live cells dominated throughout the biofilm with a certain amount of dead cells for both the CPE-K-treated one and the control (Fig. 4), indicating that the whole biofilm was metabolically active. There was no difference in cell spatial viability between the CPE-K treated biofilm and the controls, indicating that adding CPE-K did not adversely affect the cell viability of *G. sulfurreducens* biofilms. Moreover, the biofilm with CPE-K addition was thicker (~40 μm) than the control (~20 μm) (Fig. 4), in accordance with the result that the CPE-K added BESs had higher biomass content than the controls (Fig. 2A). Therefore, addition of CPE-K helped the accumulation of *G. sulfurreducens* cells on the anode surface

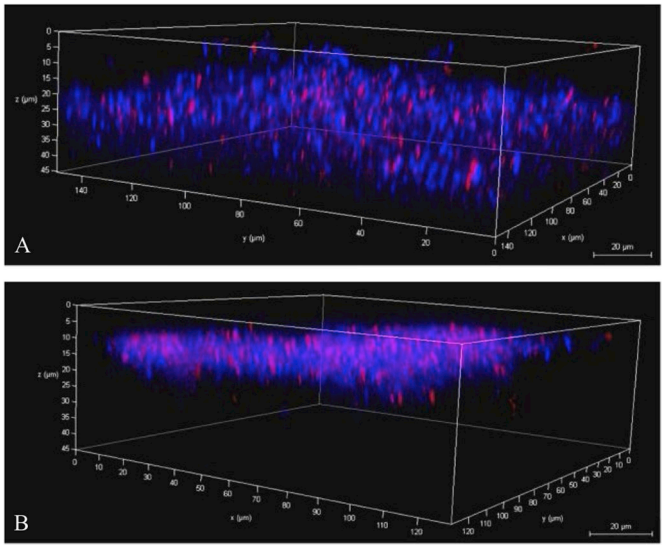

Fig. 4. Top down 3D spatial images of *G. sulfurreducens* biofilm at the end of cycle 20 in Fig. 1A, (A) biofilm with CPE-K addition and (B) control biofilm. Biofilm were TOTAL/DEAD viability stained, and observed by confocal scanning microscopy. Total cells were imaged as blue, while dead cells were imaged here as pink. (For interpretation of the references to color in this figure legend, the reader is referred to the Web version of this article.)

to form thick biofilms without impairing the metabolic activity.

The permeability of *G. sulfurreducens* biofilms was evaluated by the diffusion of fluorescein into the biofilm in a fixed amount of time after staining and visualized using confocal scanning microscope. The profiles of fluorescein inside the biofilms were quite different between the CPE-K treated BES and the control. For the biofilm with CPE-K addition, fluorescein penetrated the entire thickness of the biofilm (Fig. 5A) and the intensity was evenly distributed with the highest concentration in the middle of the biofilm (Fig. 5C). In contrast, the fluorescein was constrained within the top 5 μm in the control biofilm (Fig. 5B), and the intensity dropped dramatically with the depth into the biofilm after reaching the peak at the surface layer (Fig. 5D). Compared with the control, the biofilm with CPE-K addition showed higher permeability indicated by the deeper penetration of fluorescein inside the biofilm. Thus, the addition of CPE-K fostered the formation of the *G. sulfurreducens* biofilm with increased permeability to allow easier diffusion of substances, explaining the lower specific diffusion resistance identified using EIS (Fig. 3B) and the sustained cell viability in the inner layer of a thicker biofilm on the CPE-K treated anode (Fig. 4).

3.5. Effect of anode potential and CPE-K concentration

Eight additional BES reactors were run in duplicate at the higher anode potential of +0.3 V and/or the higher CPE-K concentration of 100 μM, with two at 0 V with 100 μM CPE-K, two at +0.3 V with 10 μM CPE-K, two at +0.3 V with 100 μM CPE-K and two controls at +0.3 V. The maximum current density produced at the stable performance stage is summarized in Fig. 6. At anode potential of 0 V, the maximum current density produced by the BESs with 10 μM CPE-K addition was 11.0 ± 0.6 A/m^2, comparable to that with 100 μM CPE-K addition (11.6 ± 0.9 A/m^2) (Fig. 6). Similarly, the maximum current density was also comparable between the BESs with 10 μM CPE-K addition (10.9 ± 0.9 A/m^2) and with 100 μM CPE-K addition (10.8 ± 0.8 A/m^2) at anode potential of +0.3 V (Fig. 6). As expected, the controls had comparable maximum current density at anode potential of 0 V (6.1 ± 0.5 A/m^2) and +0.3 V (5.6 ± 1.1 A/m^2) (Fig. 6) (Wei et al., 2010; Zhu et al., 2012). Regardless of the anode potentials and CPE-K concentrations tested, the CPE-K treated BESs showed comparable maximum current density, being two-fold that of the controls. This

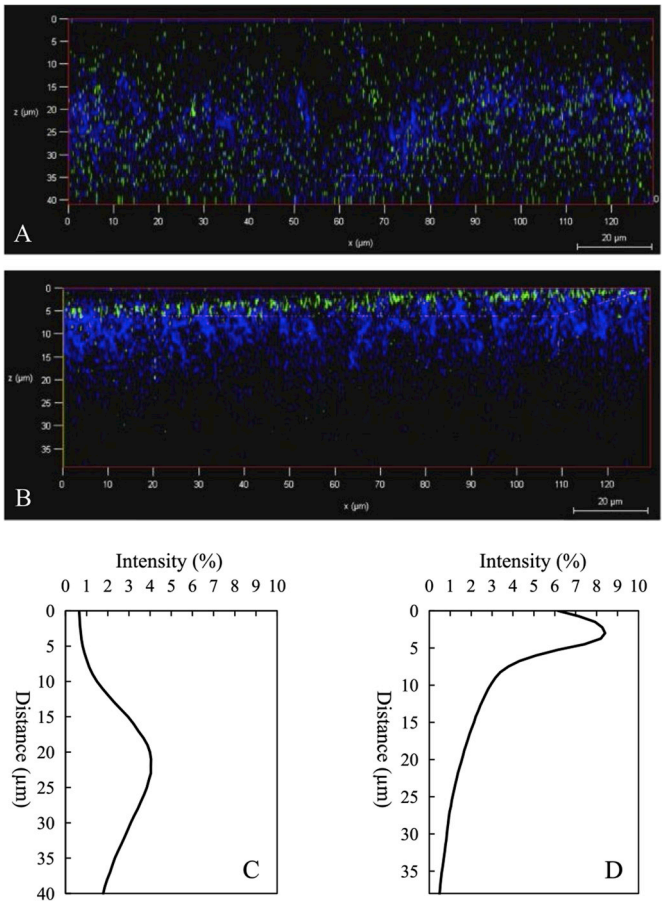

Fig. 5. Images of xz sections of anode biofilm of *G. sulfurreducens* at the end of cycle 20 in Fig. 1A showing the diffusion of fluorescein, (A) biofilm with CPE-K addition and (B) control biofilm. Profiles of the relative intensity of fluorescein at different positions of the biofilm in the images, (C) biofilm with CPE-K addition and (D) control biofilm.

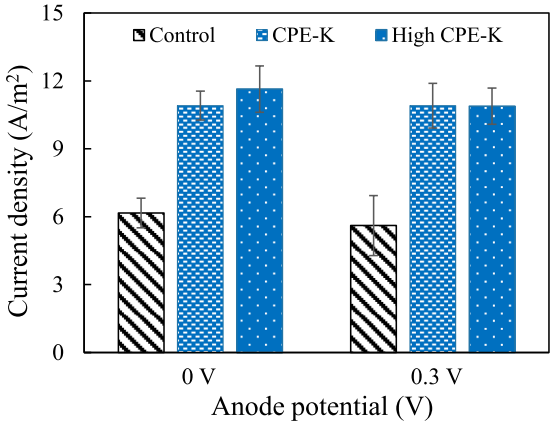

Fig. 6. Maximum current density produced by *G. Sulfurreducens* biofilm in BESs with CPE-K addition and the controls at different anode potentials and under different CPE-K concentrations. "CPE-K" indicates the BESs treated with 10 μM CPE-K, and "High CPE-K" indicates the ones treated with 100 μM CPE-K. The error bars stand for the standard deviation of at least duplicates with CPE-K addition and of the controls.

suggested that the enhancement in current production did not require the electrochemical oxidation of CPE-K at the reported redox potential of +0.27 V versus Ag/AgCl (Kirchhofer et al., 2017b; Mai et al., 2013). To our surprise, the further enhanced electricity production coupled by the redox process of CPE-K at higher electrode potential of +0.3 V with *S. oneidensis* did not happen to *G. sulfurreducens* as we anticipated.

4. Discussion

Addition of CPE-K during the formation of *G. sulfurreducens* biofilms increased maximum current density by almost one-fold in BESs (Figs. 1 and 6). The increased current density resulted from improved biofilm properties, in terms of biomass content and biofilm permeability. Firstly, CPE-K enhanced cell affinity and agglutination by virtue of being a hydrophilic conductive organic polymer. Electrochemical analyses using EIS showed that CPE-K addition decreased the charge transfer resistance at the interface of the bacterial cell and the electrode (Fig. 3A), as a result of enhanced cell affinity and electronic coupling with the graphite electrode surface (Liu et al., 2010). The biomass measurements showed that the biomass content of the CPE-K treated BESs was much higher than that of the controls due to better cell agglutination with the presence of CPE-K (Fig. 2A). Previous work also demonstrated that CPE-K facilitates the extracellular electron transfer and enhances cell assembly on electrode surface for *S. oneidensis* in BES (Kirchhofer et al., 2017b).

Secondly, CPE-K treatement increased the permeability of *G. sulfurreducens* biofilm, as indicated by the faster diffusion of fluorescein inside the biofilm compared to the control (Fig. 5). EIS also showed a decrease in specific diffusion resistance for the CPE-K treated anode as a result of the increased biofilm permeability (Fig. 3B). As an anionic conjugated polyelectrolyte, when CPE-K was encapsulated among cells, the cells might pack less densely due to electrostatic repulsion so that the biofilm was more porous and permeable (Mashkour et al., 2016). Thus, substrate and metabolic products could readily diffuse into or out of the biofilm, leading to a metabolically active inner layer at the electrode surface even with thicker biofilms in CPE-K treated BES (Fig. 4). With the same biofilm spatial viability (Fig. 4), increased biomass content in CPE-K treated BESs meant more cells were producing electrons to be extracted. The diffusion resistance of the biofilm did not increase to the same extent as the biomass, due to decreased specific diffusion resistance by CPE-K treatment. In other words, if the thickness of the biofilm (biomass content) was the same, the CPE-K treated biofilm would have smaller diffusion resistance than the controls, leading to higher current production (Figs. S5 and S6). Along with the decreased charge transfer resistance at the cell/electrode interface, the BESs with CPE-K addition produced much higher current than the controls.

Once current density was increased by adding CPE-K, this increase in current density was sustained in subsequent cycles even when the CPE-K was no longer added to the growth medium (Fig. 1C). If the increase in current density was due to redox shuttling of CPE-K, the current density should have reduced to the level of the control when CPE-K was no longer added into the medium. Moreover, increase in current density was observed at anode potential of 0 V, where the CPE-K could not be electrochemically oxidized given its redox potential of +0.27 V (Fig. 6). This excluded that the increased BES performance was resulted from CPE-K behaving as an electron mediator as shown in previous work at higher electrode potential of +0.3 V (Kirchhofer et al., 2017b). Also, the increased current density was not due to pH or conductivity change in BESs, since the addition of CPE-K did not affect the pH of the growth medium (data mentioned above) or the solution resistance as identified by EIS (Fig. 3A). Thus, it was clear from these results that CPE-K treatment increased current production of *G. sulfurreducens* biofilm through the combination of enhanced cell affinity and improved biofilm permeability, and that there were no secondary effects of chemical reactions in solution or impairment of the biofilm spatial viability.

5. Conclusions

Adding CPE-K in *G. sulfurreducens* biofilms increased the maximum current densities produced in BESs by almost one-fold, and this increase was sustained even with no further addition of CPE-K in the growth medium. The improved performance resulted from increased biomass growth, decreased charge transfer resistance at the cell/electrode interface, along with mitigated diffusion resistance. Once CPE-K was encapsulated among the *G. sulfurreducens* cells to form a biofilm on the carbon electrode surface, its distinct chemical structure led to strengthened cell affinity and agglutination, better electronic coupling between the cells and the electrode surface, and a more permeable biofilm structure with enhanced mass transport ability. The electrochemical process affiliated with CPE-K at higher electrode potentials seen with *S. oneidensis* did not occur with *G. sulfurreducens* biofilms as we anticipated. However, certain properties of the biofilm have been augmented with CPE-K to give increased current production by *G. sulfurreducens* biofilm in BES.

Declaration of competing interest

The authors declare that they have no known competing financial interests or personal relationships that could have appeared to influence the work reported in this paper.

Acknowledgements

We acknowledge the use of the NRI-MCDB Microscopy Facility and the Resonant Scanning Confocal at University of California, Santa Barbara supported by NSF MRI grant 1625770. This work was supported by the Camille and Henry Dreyfus Foundation through University of California, Santa Barbara (UCSB).

Appendix A. Supplementary data

Supplementary data to this article can be found online at https://doi.org/10.1016/j.bios.2019.111630.

References

Armand, M., Endres, F., MacFarlane, D.R., Ohno, H., Scrosati, B., 2009. Nat. Mater. 8, 621.
Balch, W.E., Fox, G.E., Magrum, L.J., Woese, C.R., Wolfe, R.S., 1979. Microbiol. Rev. 43, 260.
Bond, D.R., Lovley, D.R., 2003. Appl. Environ. Microbiol. 69, 1548.
Call, D.F., Logan, B.E., 2011. Biosens. Bioelectron. 26, 4526.
Call, D.F., Wagner, R.C., Logan, B.E., 2009. Appl. Environ. Microbiol. 75, 7579.
Cheng, S.-A., Xing, D.-F., Logan, B.E., 2011. Biosens. Bioelectron. 26, 1913.
Franks, A.E., Nevin, K.P., Glaven, R.H., Lovley, D.R., 2010. ISME J. 4, 509.
Guo, K., Freguia, S., Dennis, P.G., Chen, X., Donose, B.C., Keller, J., Gooding, J.J., Rabaey, K., 2013. Environ. Sci. Technol. 47, 7563.
Hou, H.-J., Chen, X.-F., Thomas, A.W., Catania, C., Kirchhofer, N.D., Garner, L.E., Han, A., Bazan, G.C., 2013. Adv. Mater. 25, 1593.
Ivanov, I., Ren, L.-J., Siegert, M., Logan, B.E., 2013. Int. J. Hydrogen Energy 38, 13135.
Kato, S., Nakamura, R., Kai, F., Watanabe, K., Hashimoto, K., 2012. Environ. Microbiol. 12, 3114.
Kirchhofer, N.D., McCuskey, S.R., Mai, C.K., Bazan, G.C., 2017b. Angew. Chem. Int. Ed. 56, 6519.
Kirchhofer, N.D., Rengert, Z.D., Dahlquist, F.W., Nguyen, T.Q., Bazan, G.C., 2017a. Chem 2, 240.
Kumar, R., Singh, L., Zularisam, A.W., 2016. Reneew. Sust. Energ. Rew. 56, 1322.
Lanthier, M., Gregory, K.B., Lovley, D.R., 2008. FEMS Microbiol. Lett. 278, 29.
Le Bideau, J., Ducros, J.B., Soudan, P., Guyomard, D., 2011. Adv. Funct. Mater. 21, 4073.
Li, S., Cheng, C., Thomas, A., 2017. Adv. Mater. 29, 1602547.
Li, N., Kakarla, R., Moon, J.-M., Min, B., 2015. J. Microbiol. Biotechnol. 25, 1114.
Liu, Y., Kim, H., Franklin, R., Bond, D.R., 2010. Energy Environ. Sci. 3, 1782.
Logan, B.E., 2009. Nat. Rev. Microbiol. 7, 375.
Logan, B.E., Rabaey, K., 2012. Science 337, 686.
Lovley, D.R., 2012. Annu. Rev. Microbiol. 66, 391.
Malvankar, N.S., Lovley, D.R., 2015. Electronic conductivity in living biofilms: physical meaning, mechanisms, and measurement methods. In: Beyenal, H., Babauta, J.T. (Eds.), Biofilms in Bioelectrochemical Systems: from Laboratory Practice to Data Interpretation. Wiley, NJ, pp. 232.
Malvankar, N.S., Tuominen, M.T., Lovley, D.R., 2012. Energy Environ. Sci. 5, 5790.
Mai, C.K., Zhou, H., Zhang, Y., Henson, Z.B., Nguyen, T.-Q., Heeger, A.J., Bazan, G.C., 2013. Angew Chem. Int. Ed. Engl. 52, 12874.
Mashkour, M., Rahimnejad, M., Mashkour, M., 2016. J. Power Sources 325, 322.
Nevin, K.P., Richter, H., Covalla, S.F., Johnson, J.P., Woodard, T.L., Orloff, A.L., Jia, H., Zhang, M., Lovley, D.R., 2008. Environ. Microbiol. 10, 2505.
Olabi, A.G., 2012. Energy 39, 2.
Olabi, A.G., 2013. Energy 61, 2.
Olabi, A.G., 2014. Energy 77, 1.
Patil, S.A., Hasan, K., Leech, D., H-gerh-ll, C., Gorton, L., 2012. Chem. Commun. 48, 10183.
Renslow, R.S., Babauta, J.T., Majors, P.D., Beyenal, H., 2013. Energy Environ. Sci. 6, 595.
Sun, D., Chen, J., Huang, H.-B., Liu, W.-F., Ye, Y.-L., Cheng, S.-A., 2016. Int. J. Hydrogen Energy 41, 16523.
Springer, T.E., Raistrick, I.D., 1989. J. Electrochem. Soc. 136, 1594.
Wang, H., Luo, H., Fallgren, P.H., Jin, S., Ren, Z.-J., 2015. Biotechnol. Adv. 33, 317.
Wei, J., Liang, P., Cao, X., Huang, X., 2010. Environ. Sci. Technol. 44, 3187.
Wen, Q., Kong, F.-Y., Ma, F., Ren, Y.-M., Pan, Z., 2011. J. Power Sources 196, 899.
Yang, L., Deng, W.-F., Zhang, Y.-.M., Tan, Y.-M., Ma, M., Xie, Q.-J., 2017. Biosens. Bioelectron. 91, 644.
Yang, M., Choi, B.G., Jung, S.C., Han, Y.-K., Huh, Y.S., Lee, S.B., 2014. Adv. Funct. Mater. 24, 7301.
Zhang, F., Pant, D., Logan, B.E., 2011a. Biosens. Bioelectron. 30, 49.
Zhang, G.-D., Zhao, Q.-L., Jiao, Y., Zhang, J.-N., Jiang, J.-Q., Ren, N.-Q., Kim, B.-H., 2011b. J. Power Sources 196, 6036.
Zhu, X.-P., Matthew, D.Y., Logan, B.E., 2012. Electrochem. Commun. 22, 116.